XI ECCOMAS Thematic Conference on Smart Structures and Materials
SMART 2025
M. Krommer, M. Nader and M. Schagerl (Eds)

Received: 1 January 2025 / Revised: 1 July 2025 / Accepted: 15 July 2025

MODELING AND DAMAGE DETECTION IN SYSTEMS WITH MULTIPLE OPERATIONAL REGIMES THROUGH A BAYESIAN MULTI-MODEL TIME SERIES APPROACH

CASPER A. DRANGSFELDT*, LUIS D. AVENDAÑO-VALENCIA* AND MARIE LÜTZEN*

*Institute of Mechanical and Electrical Engineering, University of Southern Denmark
Campusvej 55, 5230 Odense, Denmark
e-mail: cadra@sdu.dk

Abstract. Vibration-based Structural Health Monitoring (SHM) has been extensively studied for decades; however, developing robust algorithms is challenging when the underlying system operates under multiple operational regimes. The dynamic characteristics of these systems are observed as multiple discrete regimes, each with a significant effect on the vibration response features, which likewise appear as multiple discrete regimes in the feature space. Hence, the development of practical SHM algorithms requires appropriate modeling of the system across operational regimes. To address this challenge, this study proposes a Bayesian Multi-model approach for damage detection. The approach utilizes time-series models for each operating regime, with the Bayesian framework constructing probability distribution models based on available data. During the inspection phase, a time-series model is fitted to newly acquired data and compared against established reference models. The closest match provides an indication of the current operating regime, while deviations serve as an damage indicator. To demonstrate this approach, a Finite Element (FE) model simulating an output shaft on a ship is used, subjected to three distinct axial load states to represent different operational regimes. Results show that the Multi-model approach can detect propagating damage at an early stage, precisely accounting for operational variability. Therefore, the proposed Multi-model effectively improves the reliability of damage detection in systems with changing operational conditions.

Key words: Structural Health Monitoring, Bayesian Autoregressive Models, Operational Variability, Damage Detection, Hamiltonian Monte Carlo

1 INTRODUCTION

The concept of damage detection of a system can be simplified to the process of comparing measurable quantities, referred to as *Damage Sensitive Features* (DSFs), to a baseline representing the expected behaviour of these DSFs under healthy conditions. Deviations from this

baseline are then used as damage indicators [1]. However, when the dynamic characteristics change, DSFs can be altered in ways similar to damage. If the changing dynamic characteristics of a system can be described through multiple operating regimes, each with unique dynamic characteristics, one approach is to define an expected behaviour of the DSFs for each operating regime. By doing so, the process of damage detection is extended. First, DSFs are extracted at a given time. Then, the operating regime which the system is operating in at the given time is classified. Lastly, the extracted DSFs are compared with the expected behaviour for the classified operating regime.

For a system in which operation is divided into multiple regimes, accurately classifying the current operating regime is crucial, as the DSFs must be compared to a baseline with similar dynamic characteristics. An approach proposed in [2] utilizes the *Gaussian Mixture Model Random Coefficient* (GMM-RC) to predict various damage scenarios in a wind turbine based on the *GMM-RC Marginal Likelihood* (GMM-RC-ML) which is analogous to classifying operating regimes. Another approach proposed in [3] employs a *Switching Vector AutoRegressive* (SVAR) model to mitigate the effects of environmental variability in both simulated and experimental setups of a building. In this approach, the full range of measured environmental parameters is divided into distinct regimes, analogous to operating regimes. Then, an AR model is used to describe the expected behaviour of each regime. In [4], a methodology is proposed for detecting small levels of structural degradation in railway suspensions subjected to various travelling speeds. The methodology establishes a Multiple Model framework, where the dynamics of the system are modeled for different operational conditions using *Transmittance Function* AR with *eXogenous* input (TF-ARX) models. When new data is obtained, a new TF-ARX model is fitted. The Kullback-Leibler divergence is then used as a distance measure between the newly fitted TF-ARX model and those in the Multiple Model. If the smallest deviation between the new model and the models in the Multiple Model exceeds a predefined threshold, it suggests the presence of structural degradation in the railway suspension. Approaches such as the SVAR model in [3] and the Multiple Model framework in [4] leverages the chosen features for both classification and further analysis, ensuring that the classification reflects the actual analysis. This is advantageous since it focuses on factors influencing the problem itself rather than on variations in operating conditions from a different perspective.

Defining the expected behaviour of DSFs under healthy conditions is crucial for ensuring statistical robustness and reliability. If the system operates under significant variability, the behaviour of DSFs will also vary accordingly. Furthermore, precise classification is essential for comparing DSFs of an unknown structural state with their expected behaviour under similar dynamic characteristics. Therefore, an approach which leverages DSFs for both classification and damage detection ensures that the classification reflects the varying dynamic characteristics. Moreover, it simplifies the process of ensuring statistical robustness and reliability by using the same DSFs for both purposes, rather than relying on separate feature sets.

This study aims to develop a Bayesian Multi-model approach for damage detection under

varying operating regimes. The proposed framework establishes individual time-series models for the vibration response characteristics at specific operating regimes. Then, a Bayesian formulation is utilized to construct probability distributions for each regime based on available data, where a *Hamiltonian Monte Carlo* (HMC) approach is employed to optimize the parameters and hyperparameters of the Bayesian model. During the inspection phase, new data is analyzed by fitting a time-series model and comparing it against the established reference models. The closest match identifies the current operating regime, while deviations indicate potential structural damage. To demonstrate the approach, a *Finite Element* (FE) model simulating an output shaft on a ship, connecting an engine to a transmission, is used. The shaft is modeled with coupled axial and lateral degrees of freedom to capture realistic interactions between axial loading and transverse displacement. Three distinct axial load states (low, medium, and high) represent different operational regimes. Then, *Autoregressive* (AR) models are fitted to time-series from each load state using HMC, and the resulting Multi-model framework is applied for damage detection.

2 METHODS

The methodology of the proposed Multi-model for a system with varying operating regimes is illustrated in Fig. 1. Given a discrete time-series of finite length, $y[t]$, DSFs are estimated to represent the unknown structural state of the system, denoted as $\boldsymbol{\Theta}_u$. Next, $\boldsymbol{\Theta}_u$ is compared to every instance within the reference model, $\mathcal{M}$, which contains multiple sets of DSFs for each operating regime, representing the system's healthy structural state. The closest match determines the operating regime active at the time $\boldsymbol{\Theta}_u$ was estimated. Finally, the deviation from the closest match is used to assess potential damage.

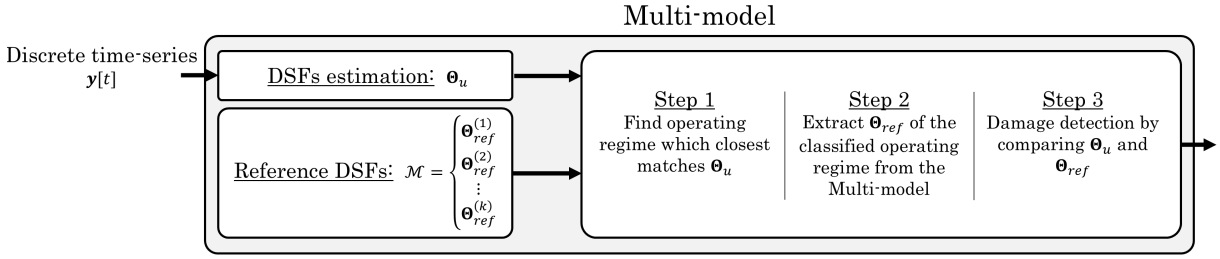

Figure 1: Flowchart of the proposed Multi-model.

The methods included in the Multi-model approach comprises estimation of the chosen DSFs and Step 1-3 as shown in Fig. 1. Therefore, the following section first details *Autoregressive modeling* (Sec. 2.1) and then AR model estimation using *Hamiltonian Monte Carlo* (Sec. 2.2). The parameters of an AR model then constitute DSFs. Lastly, the structure of the *Multi-model approach* (Sec. 2.3) is detailed, including the reference model $\mathcal{M}$ and Steps 1–3 in Fig. 1.

2.1 Autoregressive modeling

AR models are a class of statistical models used to generate a parameterized representation of discrete time-series data. In an AR model, the current value of the discrete time-series is expressed as a linear combination of its previous values and a stochastic error term. Mathematically, an AR model is defined as:

$$y[t] = -\sum_{i=1}^{n_a} a_i \cdot y[t-i] + w[t], \quad w[t] \sim NID(0, \sigma_w^2) \tag{1}$$

where $w[t]$ is *Normally and Independently Distributed* (NID) with zero mean and variance σ_w^2. This term is referred to as the *innovations* which account for the part of the discrete time-series that cannot be predicted from its previous values. The model order, n_a, determines the number of time lags included to predict future values [1]. The AR model can be written compactly as:

$$y[t] = \boldsymbol{\Phi}^T[t] \cdot \boldsymbol{\theta} + w[t], \quad \text{with} \quad \boldsymbol{\Phi}[t] = \begin{bmatrix} y[t-1] \\ y[t-2] \\ \cdots \\ y[t-n_a] \end{bmatrix} \quad \text{and} \quad \boldsymbol{\theta} = \begin{bmatrix} a_1 \\ a_2 \\ \cdots \\ a_{n_a} \end{bmatrix} \tag{2}$$

where $\boldsymbol{\Phi}$ is the design matrix and $\boldsymbol{\theta}$ is the AR parameter vector.

The model parameters, $\boldsymbol{\theta}$ and σ_w^2, are modeled as random variables conditioned on the operating regimes. Applying Bayes' theorem, the inference problem for an AR model in each operating regime is written as:

$$p\left(\boldsymbol{\theta}, \sigma_w^2 | \boldsymbol{y}, \boldsymbol{\Phi}\right) = \frac{p\left(\boldsymbol{y}|\boldsymbol{\Phi}, \boldsymbol{\theta}, \sigma_w^2\right) p\left(\boldsymbol{\theta}|\sigma_w^2\right) p\left(\sigma_w^2\right)}{p\left(\boldsymbol{y}|\boldsymbol{\Phi}\right)} \tag{3}$$

where $\boldsymbol{y}$ and $\boldsymbol{\Phi}$ represent the observations and the lagged observations respectively. Computation of the posterior $p\left(\boldsymbol{\theta}, \sigma_w^2 | \boldsymbol{y}, \boldsymbol{\Phi}\right)$ can be challenging and sometimes impossible. Therefore, the posterior is often estimated using numerical methods, such as HMC.

2.2 Hamiltonian Monte Carlo

HMC is a method derived from *Markov Chain Monte Carlo* (MCMC) simulations, where a sequence of dependent samples is generated to approximate the posterior distribution. Starting from an initial sample drawn from the parameter space, a trajectory based on the curvature in the parameter space is followed to generate a new sample. This process continues until the parameter space has been explored sufficiently.

Following the HMC approach to approximate the posterior in Eq. (3), the posterior is augmented with an independent momentum distribution, $p\left(\boldsymbol{\Theta}, \boldsymbol{\phi} | \boldsymbol{y}, \boldsymbol{\Phi}\right) = p(\boldsymbol{\phi}) p(\boldsymbol{\Theta} | \boldsymbol{y}, \boldsymbol{\Phi})$, where $\boldsymbol{\Theta} = \{\boldsymbol{\theta}, \sigma_w^2\}$ is referred to as the position in the parameter space, and $\boldsymbol{\phi}$ is the momentum.

The momentum dimension matches that of the latent variables, and its distribution is typically chosen as a multivariate normal, $\boldsymbol{\phi} \sim \mathcal{N}(0, \boldsymbol{\Sigma})$. The concept of augmenting the true posterior with a momentum origins from Hamiltonian mechanics, where the total energy of the *system* can be described as:

$$H(\boldsymbol{\Theta}, \boldsymbol{\phi}) = U(\boldsymbol{\Theta}) + K(\boldsymbol{\phi}) \tag{4}$$

Here, the potential energy of the system corresponds to the negative log-posterior and the kinetic energy relates to the momentum distribution, both described as:

$$U(\boldsymbol{\Theta}) = -\log p(\boldsymbol{\Theta}|\boldsymbol{y}, \boldsymbol{\Phi}), \quad K(\boldsymbol{\phi}) = \frac{1}{2}\boldsymbol{\phi}^T \boldsymbol{\Sigma}^{-1} \boldsymbol{\phi} \tag{5}$$

where $U(\boldsymbol{\Theta})$ represents the 'height' in the parameter space, with areas of high probability density corresponding to greater potential energy. The kinetic energy, $K(\boldsymbol{\phi})$, represents the 'speed' of movement through the parameter space. The trajectory through the parameter space to draw new samples is then governed by Hamiltonian dynamics. Here, leapfrog integration is often utilized to discretize the trajectories in time [5].

The leapfrog integration alternately updates the position $\boldsymbol{\Theta}$ and momentum $\boldsymbol{\phi}$ over L steps, referred to as leapfrog steps, with each step scaled by the stepsize ϵ. After L steps, the new position $\boldsymbol{\Theta}$ represents a potential new sample in the parameter space. Before accepting this new position, an accept-reject step is performed. The acceptance ratio is computed as:

$$r = \frac{p(\boldsymbol{\Theta}^*|\boldsymbol{y}, \boldsymbol{\Phi})p(\boldsymbol{\phi}^*)}{p(\boldsymbol{\Theta}^{t-1}|\boldsymbol{y}, \boldsymbol{\Phi})p(\boldsymbol{\phi}^{t-1})} \tag{6}$$

where $\boldsymbol{\Theta}^*$ and $\boldsymbol{\phi}^*$ are the position and momentum obtained after performing the leapfrog integration, and $\boldsymbol{\Theta}^{t-1}$ and $\boldsymbol{\phi}^{t-1}$ are the position and momentum before the leapfrog integration. The new position $\boldsymbol{\Theta}^{t-1}$ is then set as:

$$\boldsymbol{\Theta}^t = \begin{cases} \boldsymbol{\Theta}^* & \text{with probability } \min(r, 1) \\ \boldsymbol{\Theta}^{t-1} & \text{otherwise} \end{cases} \tag{7}$$

This process of drawing a new sample of $\boldsymbol{\Theta}$ is repeated iteratively until N_s accepted samples of $\boldsymbol{\Theta}$ sufficiently resemble the true posterior. The result of the simulation is an approximation of the posterior with N_s samples, $\hat{p}(\boldsymbol{\Theta}|\boldsymbol{y}, \boldsymbol{\Phi})$ where $\boldsymbol{\Theta} \in \mathbb{R}^{N_s \times (n_a+1)}$.

In general, the simulation starts at an initial position $\boldsymbol{\Theta}_0$ and a random momentum drawn from its distribution. From this starting point, the leapfrog integration is performed with L steps to propose a new position, thereby a new sample. If the new position is accepted, the simulation proceeds from this updated position; otherwise, it resumes from the previous position. Independent if the position is updated, $\boldsymbol{\phi}$ is resampled. The parameters of the HMC approach are either tuned manually or adjusted using adaptive methods [5].

2.3 Multi-model approach

Defining the Multi-model requires multiple datasets of the system in a healthy state across all regimes to capture the full variability in DSFs under healthy conditions. Therefore, given the i^{th} subset of data while operating in the k^{th} regime, the posterior $p(\boldsymbol{\Theta}|\boldsymbol{\mathcal{D}}_i^{(k)})$ is approximated with N_s samples where the i^{th} subset of data is denoted as $\boldsymbol{\mathcal{D}}_i^{(k)} = \{\boldsymbol{y}_i^{(k)}, \boldsymbol{\Phi}_i^{(k)}\}$. Then, the Multi-model can be written as:

$$\boldsymbol{\mathcal{M}} = \begin{cases} \hat{p}(\boldsymbol{\Theta}|\boldsymbol{\mathcal{D}}_1^{(1)}) & \hat{p}(\boldsymbol{\Theta}|\boldsymbol{\mathcal{D}}_2^{(1)}) & \cdots & \hat{p}(\boldsymbol{\Theta}|\boldsymbol{\mathcal{D}}_{N_1}^{(1)}) \\ \hat{p}(\boldsymbol{\Theta}|\boldsymbol{\mathcal{D}}_1^{(2)}) & \hat{p}(\boldsymbol{\Theta}|\boldsymbol{\mathcal{D}}_2^{(2)}) & \cdots & \hat{p}(\boldsymbol{\Theta}|\boldsymbol{\mathcal{D}}_{N_2}^{(2)}) \\ \vdots & & & \\ \hat{p}(\boldsymbol{\Theta}|\boldsymbol{\mathcal{D}}_1^{(k)}) & \hat{p}(\boldsymbol{\Theta}|\boldsymbol{\mathcal{D}}_2^{(k)}) & \cdots & \hat{p}(\boldsymbol{\Theta}|\boldsymbol{\mathcal{D}}_{N_k}^{(k)}) \end{cases} \tag{8}$$

where N_1, N_2, and N_k denote the number of data subsets available for each operating regime.

Once the Multi-model is defined , the first step is to classify the operating regime of the system given a new set of DSFs, $\hat{p}(\boldsymbol{\Theta}|\boldsymbol{\mathcal{D}}_u)$ where u denotes that the structural state of the system is unknown. The classification is performed by comparing the parameters $\boldsymbol{\Theta}_u$ in $\hat{p}(\boldsymbol{\Theta}|\boldsymbol{\mathcal{D}}_u)$ to each reference $\boldsymbol{\Theta}_i^{(k)}$ in $\hat{p}(\boldsymbol{\Theta}|\boldsymbol{\mathcal{D}}_i^{(k)})$ in the Multi-model. First, the squared difference between $\boldsymbol{\Theta}_u$ and each reference $\boldsymbol{\Theta}_i^{(k)}$ in the Multi-model is computed and summed across all N_k:

$$\log p(k|\boldsymbol{\Theta}_u, \boldsymbol{\Theta}^{(k)}) = -\frac{1}{N_k} \sum_{i=1}^{N_k} (\boldsymbol{\Theta}_u - \boldsymbol{\Theta}_i^{(k)})^2 \tag{9}$$

where $\log p(k|\boldsymbol{\Theta}_u, \boldsymbol{\Theta}^{(k)})$ represents the log-likelihood of the system being in the k^{th} operating regime while $\boldsymbol{\Theta}_u$ was estimated. Then, the probability of the system operating under regime k is obtained by averaging the log-likelihoods across all references:

$$P_k = \frac{\exp\left(-\frac{1}{N_k}\sum_{i=1}^{N_k}(\boldsymbol{\Theta}_u - \boldsymbol{\Theta}_i^{(k)})^2\right)}{\sum_j \exp\left(-\frac{1}{N_j}\sum_{i=1}^{N_j}(\boldsymbol{\Theta}_u - \boldsymbol{\Theta}_i^{(j)})^2\right)} \tag{10}$$

where P_k represents the probability that the system is operating under regime k. Finally, the regime with the highest probability is selected as the predicted operating regime.

Subsequently, the probability of the predicted operating regime serves as a damage indicator. If $\boldsymbol{\Theta}_u$ exactly matches one of $\boldsymbol{\Theta}_i$ within the Multi-model, the probability P_k equals 1. Conversely, if $\boldsymbol{\Theta}_u$ deviates from its closest match, the probability P_k will be less than 1. Therefore, the damage detection process of the Multi-model approach is defined as:

$$\text{Healthy if:} \quad |\log P_k| \leq \vartheta \quad \text{or} \quad \text{Damaged if:} \quad |\log P_k| > \vartheta \tag{11}$$

where ϑ is a predefined threshold that determines the acceptable level of deviation.

3 CASE STUDY - DAMAGE DETECTION OF A SHAFT

The proposed Multi-model approach is applied to a simply case where the system response is simulated from a FE model. The FE model shown in Fig. 2 represents an output shaft of a Volvo IPS, which connects an engine to a transmission on a ship, transferring torque down to the propellers. The shaft is modeled as simply supported at both ends, as the connections to the engine and transmission are cardan joints. Furthermore, the connection between the shaft and the transmission can vary slightly, since the transmission is clamped to the hull of the ship using rubber mounts, allowing for some movement. This slight movement subjects the shaft to varying levels of axial loading F, depending on the operational conditions. As a result, the dynamic characteristics change over time. This justifies the use of the Multi-model approach for damage detection, as the changing dynamic characteristics are likely to alter the system response in ways similar to damage.

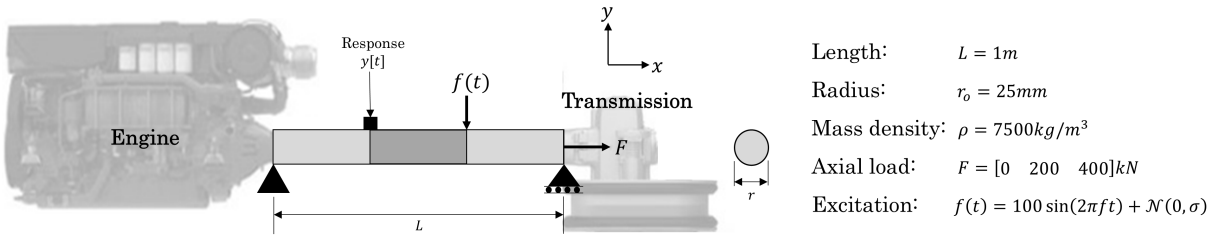

Figure 2: Simply supported beam with 3 elements subjected to transverse and axial loading.

The following details first the formulation of the FE model and the system response simulation in Sec. 3.1. Then, the modeling process of the Multi-model is detailed in Sec. 3.2.

3.1 Finite element formulation and simulation

The FE model in Fig. 2 is subjected to three levels of constant axial load F and modeled using 3 Euler-Bernoulli elements, each with element stiffness matrix defined as:

$$\boldsymbol{K}_e = \frac{EI}{l_e^3}\begin{bmatrix} 12 & 6l_e & -12 & 6l_e \\ 6l_e & 4l_e^2 & -6l_e & 2l_e^2 \\ -12 & -6l_e & 12 & -6l_e \\ 6l_e & 2l_e^2 & -6l_e & 4l_e^2 \end{bmatrix} + \frac{F}{30l_e}\begin{bmatrix} 36 & 3l_e & -36 & 3l_e \\ 3l_e & 4l_e^2 & -3l_e & -l_e^2 \\ -36 & -3l_e & 36 & -3l_e \\ 3l_e & -l_e^2 & -3l_e & 4l_e^2 \end{bmatrix} \tag{12}$$

and element mass matrix defined as [6]:

$$\boldsymbol{M}_e = \frac{\rho A l_e}{420}\begin{bmatrix} 156 & 22l_e & 54 & -13l_e \\ 22l_e & 4l_e^2 & 13l_e & -3l_e^2 \\ 54 & 13l_e & 156 & -22l_2 \\ -13l_e & -3l_e^2 & -22l_e & 4l_e^2 \end{bmatrix} \tag{13}$$

where $l_e = L/3$ is the length of each element, E is the Young's modulus, I is the moment of inertia, ρ is the mass density, A is the cross-sectional area, and F is the axial load. These parameters are given in Fig. 2 and are chosen as a rough representation of a real setup. In total, this yields a global stiffness, $\boldsymbol{K}$, and mass matrix, $\boldsymbol{M}$, with sizes 8×8. In addition, proportional damping is used modeled as:

$$\boldsymbol{C} = \alpha \boldsymbol{M} + \beta \boldsymbol{K} \tag{14}$$

where $\alpha = 10$ and $\beta = 10^{-6}$. Furthermore, the shaft is excited in a single DOF by a harmonic transverse force, $f(t)$ in Fig. 2 where $f = 10Hz$ and $\sigma = 5$. Lastly, the first and last transverse DOF are eliminated due to boundary conditions, reducing the system matrices to 6×6.

To simulate a system that transition through multiple operating regimes, a *Hidden Markov Model* (HMM) is used with the transition probability matrix:

$$\boldsymbol{A} = \begin{bmatrix} 0.85 & 0.15 & 0 \\ 0.1 & 0.8 & 0.1 \\ 0 & 0.15 & 0.85 \end{bmatrix} \tag{15}$$

This structure constrains the load sequence, ensuring that the system cannot move directly from the lowest to the highest level. Then, using the HMM, a total of 400 transitions are generated, with each segment maintaining a minimum stationary period of 5 seconds before a transition occurs in the load sequence.

The system response simulation is through a discrete state-space representation, as detailed in [7], with a sampling rate of $f_s = 4000$Hz. Additionally, damage is introduced after 900 seconds in the element marked as dark gray at the shaft in Fig. 2. Here, the element stiffness is gradually reduced from 0% to 5% over a period of 1100 seconds. During the simulation, the temperature increases linearly from 20^oC to 40^oC over the first 500 seconds, then remains stable for the next 1500 seconds. For this, the Young's modulus is modeled as temperature dependent defined roughly as $E(t) = -\frac{1}{20}\text{GPa}/^o\text{C} \cdot t + 210\text{GPa}$. This is shown at the top of Fig. 3, along with the temperature profile. The load sequence and simulated system response are also shown. Additionally, the onset of damage is indicated by a black line.

The simulation yields a subset of data when the model is undamaged, $\boldsymbol{Y}_H$ and a subset of data after the damage have been introduction, $\boldsymbol{Y}_D$:

$$\boldsymbol{Y}_H \in \mathbb{R}^{5f_s \times 180} \quad \& \quad \boldsymbol{Y}_D \in \mathbb{R}^{5f_s \times 220} \tag{16}$$

where 85% of the 180 subsets in $\boldsymbol{Y}_H$ are randomly chosen for training. The remaining 15% of subsets in $\boldsymbol{Y}_H$ and $\boldsymbol{Y}_D$ is used for testing.

3.2 Modeling process

The modeling framework of the Multi-model approach is structured into three key stages: *AR Model Selection*, *AR Model Estimation*, and *Constructing the Multi-model*.

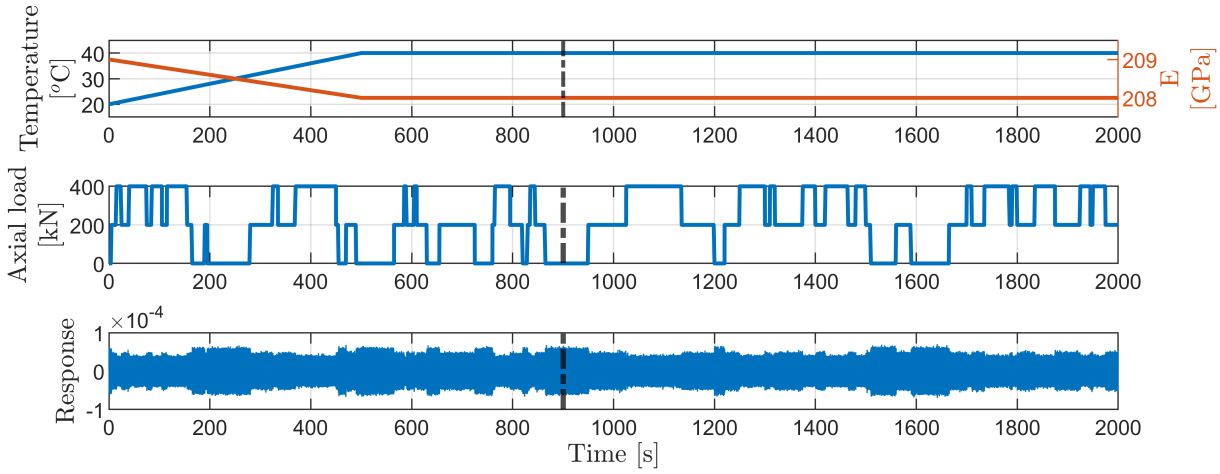

Figure 3: The system response simulation.

AR Model selection involves defining a suitable model order, n_a in Eq. (1) and setting the priors in the Bayesian inference problem in Eq. (3), along with defining a likelihood distribution. The first selection is the model order which is set to 20. This selection was based on a deterministic assessment, where the *Residual Sum of Squares over Series Sum of Squares* and the *Bayesian Informative Criterion* was evaluated for an increasing n_a while $\boldsymbol{\Theta}$ was estimated using *Least Square* (LS) estimation. The next selection is the priors and likelihood distribution. The likelihood is assumed to follow a Gaussian distribution as $p(\boldsymbol{y}|\boldsymbol{\Phi}, \boldsymbol{\theta}, \sigma_w^2) \sim N(\boldsymbol{\Phi}^T\boldsymbol{\theta}, \sigma_w^2)$. The prior distribution of the parameter vector $\boldsymbol{\theta}$ is assumed to follow a Gaussian distribution as $p(\boldsymbol{\theta}|\sigma_w^2) \sim N(\hat{\boldsymbol{\theta}}_{LS}, \sigma_w^2 \boldsymbol{I}_{n_a \times n_a})$ where $\hat{\boldsymbol{\theta}}_{LS}$ is a LS estimate of the parameters. Lastly, the prior distribution of σ_w^2 is assumed to follow an Inverse-Gamma distribution as $p(\sigma_w^2) \sim IG(2, 1)$.

AR Model estimation comprises the HMC simulation to approximate the posterior $p(\boldsymbol{\Theta}|\boldsymbol{\mathcal{D}}_i)$ given each subset in $\boldsymbol{Y}_H$ and $\boldsymbol{Y}_D$ in Eq. (16). Here, the number of accepted samples N_s to approximate the $p(\boldsymbol{\Theta}|\boldsymbol{\mathcal{D}}_i)$ is set to 5000. The remaining parameters of the HMC simulation, namely the variance of the momentum $\boldsymbol{\Sigma}$, the number of leapfrog steps L, and the step size ϵ, are tuned adaptively for each simulation.

Constructing the Multi-model involves using the estimated posteriors from the training subsets to build the Multi-model in Eq. (8). As a result, the Multi-model consists of 153 estimated posteriors, with the number of estimated posteriors for the first operating regime, N_1, being 50, while N_2 and N_3 holds 60 and 43, respectively. The posteriors are estimated both during the temperature increase and after, ensuring that the Multi-model accurately represents the system response under healthy conditions.

4 RESULTS

After the establishment of the Multi-model to represent the system response under healthy conditions, the damage detection process is tested and evaluated. For each subset in both $\boldsymbol{Y}_H$ and $\boldsymbol{Y}_D$, the parameter $\boldsymbol{\Theta}_u$ in the approximated posterior $\hat{p}(\boldsymbol{\Theta}|\boldsymbol{\mathcal{D}}_i)$ are compared with the Multi-model following Eq. (10) where the damage evaluation follows Eq. (11). The process is continued for $i \in [1, 2, \ldots, 400]$, where the damage detection for each classified operating regime is shown in Fig. 4. Here, the regions marked as *Training* comprise the approximated posteriors used to construct the Multi-model, meaning that $\boldsymbol{\Theta}_u$ matches itself within the Multi-model with a probability of 100%. The regions marked as *Testing* contain the approximated posteriors for the 15% subsets in Y_H, which are used to define the threshold ϑ in Eq. (11). This threshold is determined such that the *True Negative* (TN) rate is 100%. The regions marked as *Damaged* contain the subsets in Y_D after damage has been introduced into the simulated system response. However, only the indices exceeding the threshold ϑ indicate instances where the Multi-model successfully detects the damage.

Given the introduced threshold for a TN rate of 100%, it can be determined the level of damage introduced possible to detect by the Multi-model. For the first operating regime, the possible level of damage to detect is a stiffness reduction of $\sim$1.4%. For the second and third regime, the level is $\sim$1.5% and $\sim$0.7% respectively. In total, the damage detection following the Multi-model approach have a *True Positive* (TP) rate of 78.6% while the TN rate is 100%.

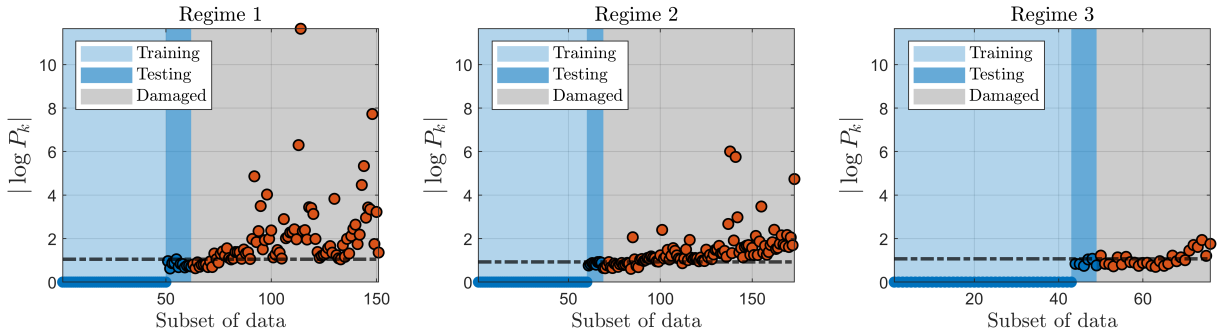

Figure 4: Damage detection following the Multi-model approach.

5 DISCUSSION

An FE model was used to simulate the system response, representing a real-case scenario where the dynamic characteristics of a system change over time. While the simple FE model provides only a rough representation of an output shaft between an engine and transmission, with geometrical dimensions that may not closely resemble any real case, the simulated response captures the changing dynamic characteristics observed in measured data. Additionally,

while the axial loading may not perfectly match real-case conditions, measured data from an actual system exhibit even greater fluctuations between operating regimes. Lastly, the load sequence consists of stationary periods of at least 5 seconds, which is rapid compared to real-case scenarios. However, the system response of a real case would likely extend over a longer duration. Overall, despite its simplicity, it is assumed that the FE model and its simulated system response provide a sufficient proof of concept for evaluating the Multi-model approach.

To represent each data subset with a duration of 5 seconds, an AR model was used, with its parameters treated as random variables and subsequently used as DSFs. While AR models directly reflect the dynamic characteristics of a system, the dimension of the model can be significant. In this controlled simulation, a large dimension is not necessary; however, in a real-case system, the dimension is likely more significant to capture complex dynamics of such system. If so, estimating the posterior could be computationally expensive, thus limiting the practical use of the proposed method if not addressed. However, dimensionality reduction methods, such as *Principle Component Analysis*, could be used, where an AR model is fitted to the features extracted from the reduction method's output, rather than directly on the time-series.

Another aspect to consider regarding the computational cost is the approximated posteriors used to define the Multi-model. In this case, an AR model was fitted to 5 seconds of data, thus resulting in a total of 153 approximated posteriors in the Multi-model. If applied to a real-case system where data for a longer duration is available, the dimension is most likely too significant. In a real-case scenario, it must be considered whether fewer AR models would be sufficient or if the time duration used for each AR model could be increased while still maintaining an accurate representation of the system. Also, having AR models in the Multi-model represent the system under different environmental conditions may prove challenging if not addressed. While varying environmental conditions influence structural dynamics in ways similar to damage, it is crucial to determine whether this also holds for the parameters of the AR models. If so, mitigation approaches must be implemented to improve damage detectability.

The damage detection approach of the proposed Multi-model is computationally inexpensive since P_k is used for both classification and as a damage indicator. Despite being a simple measure of damage, the TP rate and the level of detectable damage were sufficient. However, there may be potential for improvement. In Fig. 4, it is observed that the testing subsets do not perfectly match the approximated posteriors in the Multi-model, resulting in the early stages of damage propagation not being detected. This issue could be addressed either by improving the Multi-model's ability to represent the system more accurately or by refining the damage detection approach to account for variability in the Multi-model.

6 CONCLUSION

A Multi-model methodology was proposed for damage detection in systems with time-varying operations, where the operation can be described through multiple operating regimes. The Multi-model leverages the same features for both classification between the regimes and

for DSFs, enhancing robustness, as classification relies on the same parameters, which could otherwise challenge damage detection. The proposed Multi-model was tested on a simulated system response of a simple FE model representing a shaft connecting an engine to a transmission, subjected to three levels of axial loading. During the simulation, damage propagation was introduced to investigate the lowest detectable level of damage by the proposed Multi-model. With a conservative threshold for damage detection, resulting in a TN rate of 100%, the TP rate was found to be 78.6%. The lowest detectable damage level was a reduction in element stiffness of around 1%. Despite limitations such as high computational cost and accurate representation of the system in real-case scenarios, potential improvements were discussed. Overall, the Multi-model showed promising results and great potential, positioning it for testing on more complex systems in real-world applications.

REFERENCES

[1] C. R. Farrar and K. Worden, *Structural health monitoring: a machine learning perspective*. Wiley, 2013.

[2] L. D. Avendaño-Valencia and S. D. Fassois, "Damage/fault diagnosis in an operating wind turbine under uncertainty via a vibration response gaussian mixture random coefficient model based framework," *Mechanical Systems and Signal Processing*, vol. 91, pp. 326–353, 2017.

[3] A. Liu, L. Wang, L. Bornn, and C. Farrar, "Robust structural health monitoring under environmental and operational uncertainty with switching state-space autoregressive models," *Structural Health Monitoring*, vol. 18, no. 2, pp. 435–453, 2019.

[4] G. Vlachospyros, S. D. Fassois, and J. S. Sakellariou, "On-board vibration-based robust and unsupervised degradation detection in railway suspensions under various travelling speeds via a multiple model framework," *Vehicle System Dynamics*, vol. 62, no. 6, pp. 1446–1470, 2024.

[5] A. Gelman, *Bayesian data analysis*, 3rd ed. CRC Press, 2014.

[6] R. D. Cook and R. D. Cook, *Concepts and applications of finite element analysis*, 4th ed. Wiley, 2002.

[7] Z. Gajic, *Linear dynamic systems and signals*. Prentice Hall/Pearson Education, 2003.